KLOE Note 207, October 2005

Study of scalar mesons decays in $\pi^+\pi^-\gamma$ events

C.Bini

Universita' "La Sapienza" and INFN Roma

1. Introduction.

The radiative decay $\phi \rightarrow f_0(980)\gamma$ can be detected at KLOE through one of the two decays $f_0(980) \rightarrow \pi^+\pi^-$ or $\rightarrow \pi^0\pi^0$, the decay $f_0(980) \rightarrow KK$ with charged or neutral kaons being suppressed by phase-space and by closeness of the f_0 mass to $2m_K$. In order to find the decay $f_0(980) \rightarrow \pi^+\pi^-$, $\pi^+\pi^-\gamma$ final states with a photon at "large angle" are considered, to reduce the background due to initial state radiation (ISR) events.

The study of this decay has the following motivations:

1. to assess the $f_0(980)$ signal in a clean way (the only published analysis of this decay chain [1] doesn't give a clean signal evidence in the mass spectrum);
2. to evaluate the parameters of the $f_0(980)$, in particular the "coupling" to the ϕ and to the KK and $\pi\pi$ systems, in order to have an indication of the strange quark content in the $f_0(980)$ structure;
3. to see if any further meson (the controversial $f_0(600)$ better known as the σ meson) is needed to describe the data;
4. to compare different models for the description of the data.

In a previous note [2] the selection of $\pi^+\pi^-\gamma$ final states with a photon at "large angle" $45° < \theta < 135°$ was described, together with the determination of the selection efficiency.

In this note I describe the results of a detailed analysis of the $\pi^+\pi^-\gamma$ data with the photon at large angle. In order to extract the scalar contributions out of a very large background (the residual, still dominant ISR plus the final state radiation (FSR)), it is essential to describe the scalar contribution according to a given "model". I have used 3 different approaches for that.

In the following after a presentation of the data (sect.2 and 3) and after a brief description of the models used to fit the data (sect.4) I present the results of the fits (sect.5) and then I discuss the results (sect.6).

2. The data sample.

The event selection is described in ref.[2]. The "on-peak" data sample consists of 6.7×10^5 events corresponding to an integrated luminosity of 350 pb^{-1} from the 2001 and 2002 data taking, at center of mass energies $\sqrt{s}$, in the range 1019.1 – 1020.3 MeV. The two "off-peak" samples consist of 6.58 and 4.93 pb^{-1} taken at 1017 and 1022 MeV respectively. Fig.1 shows the $\pi\pi$ invariant mass spectrum (*m* in the following) in the full kinematically allowed energy range from the threshold ($2m_\pi$ = 278 MeV) up to the ϕ mass, in 1.2 MeV wide bins for the "on-peak" sample. The *m* spectra for "off-peak" data in bins of 6 MeV are shown in fig.2.

In fig.3 the "on-peak" *m* spectrum is compared with the small angle analysis ($\theta < 15^o$) spectrum [3]. Notice the acceptance cut in the small angle spectrum at about 550 MeV and the larger rate in the ρ-ω region. Notice also that in the small angle region the $\phi \rightarrow S\gamma$ contribution is expected to be reduced by a factor $\int_{LA}(1+\cos^2\theta)d\cos\theta / \int_{SA}(1+\cos^2\theta)d\cos\theta \sim 12$ while the ISR contribution is increased by a factor ~5. The relative contribution of the scalar amplitude in the small angle region is reduced by a factor ~60 respect to the large angle.

The data have been divided in slices of centre of mass energy. For each slice, the number of events in the 900-1000 MeV invariant mass region normalized to the integrated luminosity provides the visible cross-section. Fig.4 shows the centre of mass energy dependence of the visible cross-section. The blue points are the "on-peak" data the red points are the "off-peak" data.

We have also considered the charge asymmetry of the two pions. We define the charge asymmetry as (θ^+ is the polar emission angle of the π^+);

$$A = \frac{N(\theta^+ > 90^o) - N(\theta^+ < 90^o)}{N(\theta^+ > 90^o) + N(\theta^+ < 90^o)}$$

A sizeable charge asymmetry is expected due to the interference between the initial state radiation and the final state radiation amplitudes that give $\pi\pi$ states of opposite charge conjugation. Infact a

large charge asymmetry is observed. Fig.5 shows the dependence of the observed charge asymmetry A as a function of *m* for the "on-peak" data. Finally fig.6 shows the charge asymmetry for the two off-peak data samples.

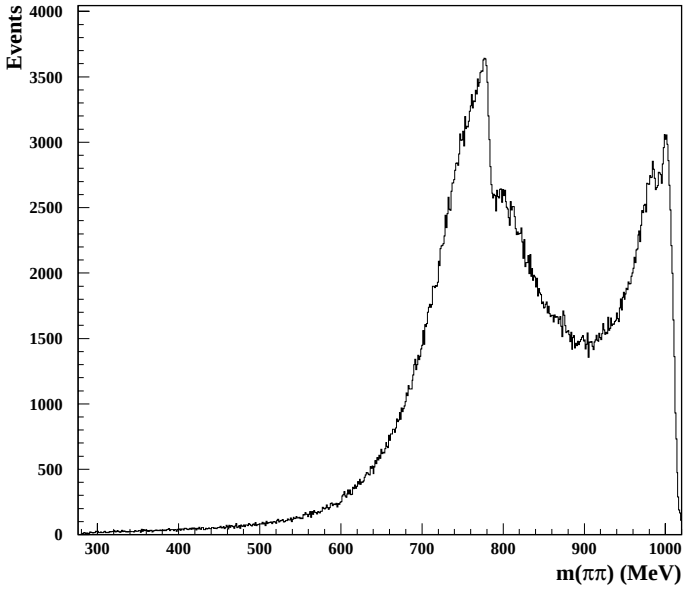

Figure 1. ππ invariant mass spectrum for the full "on-peak" data sample.

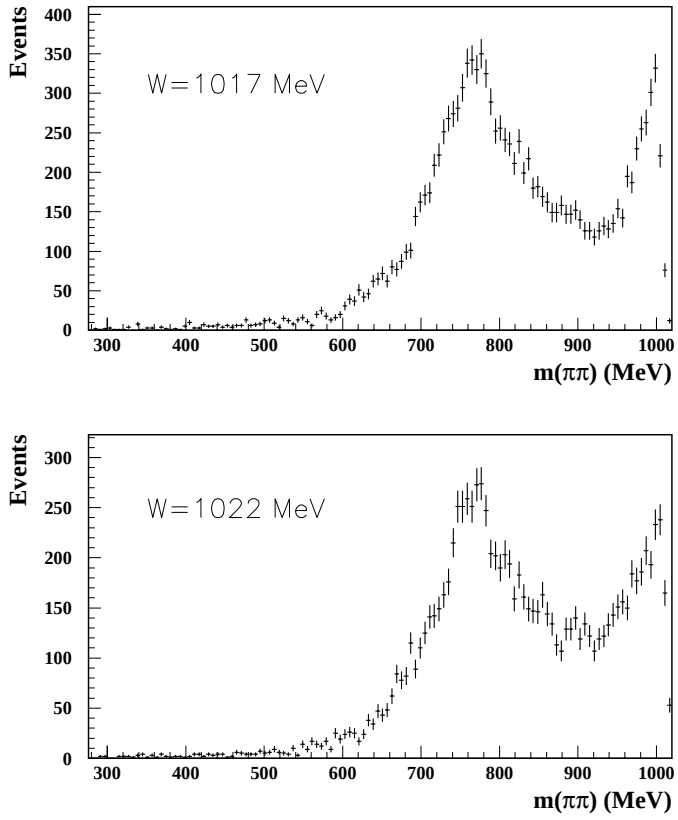

Figure 2. ππ invariant mass spectra for the two "off-peak" data samples.

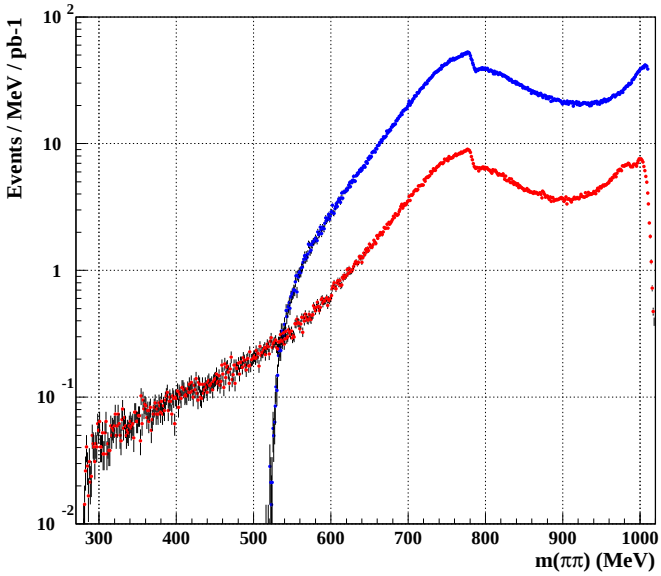

Figure 3. Comparison of the large angle spectrum (red, the same of fig.1) and the small angle spectrum (blue).

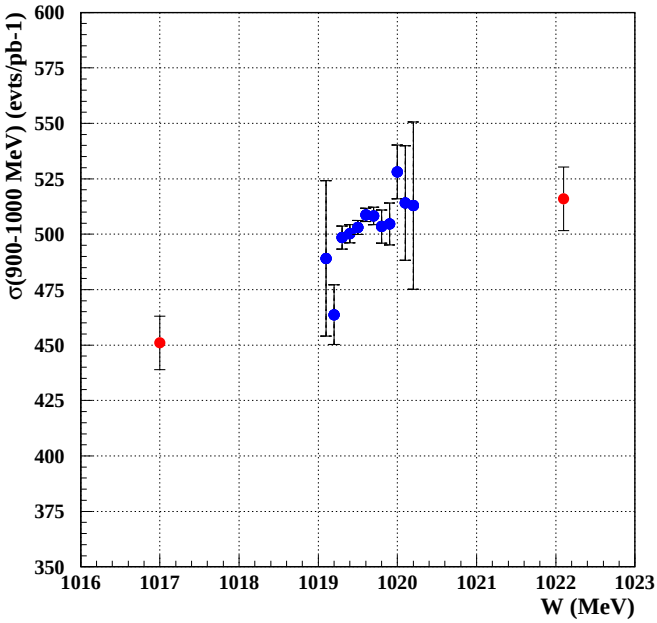

Figure 4. Centre of mass energy (W = √s) dependence of the visible cross-section for events with a ππ invariant mass in the range 900 - 1000 MeV. The blue points are the "on-peak" data sliced in W, the red points are the two "off-peak" samples.

Figs.1 and 5 give in an independent way a clear evidence of a signal in the 900-1000 MeV region that can be easily attributed to the effect of the $f_0(980) \rightarrow \pi^+\pi^-$.
In the following the attention will be focussed mainly on the mass spectrum of the "on-peak" data, where a detailed fit procedure has been applied. "Off-peak" data are compared with extrapolations based on the fit results at the peak (see sect.6.4), but are not included in the fit.

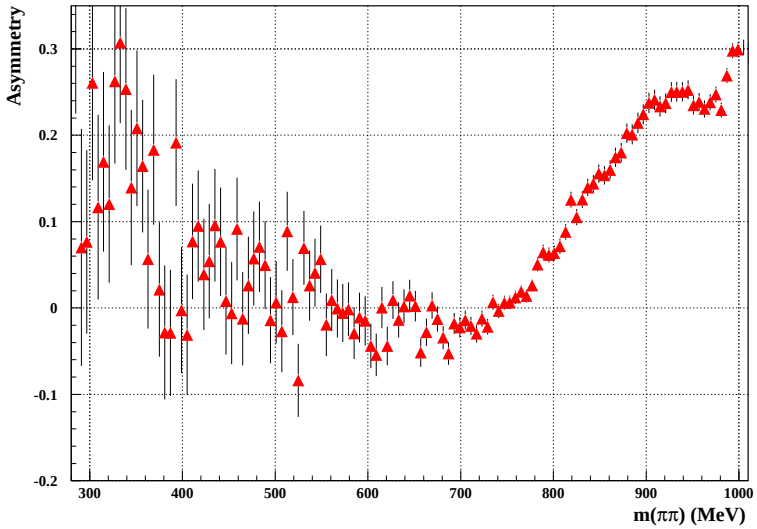

Figure 5. Charge asymmetry as a function of *m* for the on-peak data sample.

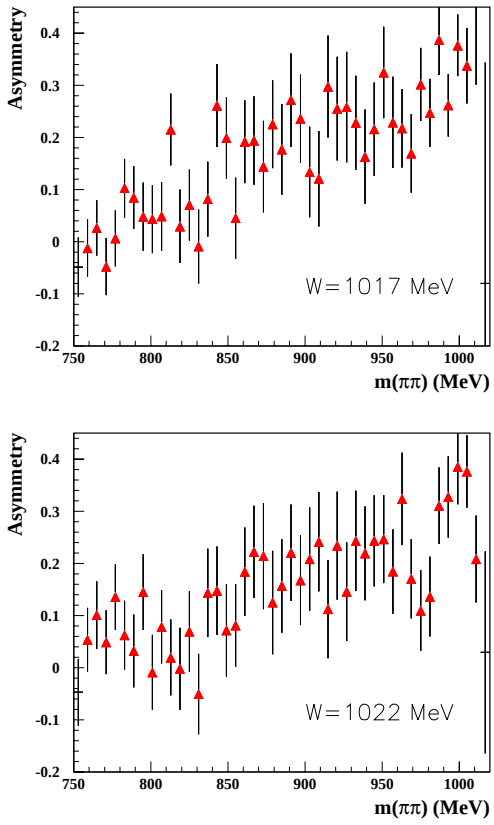

Figure 6. Charge asymmetry as a function of *m* for the two "off-peak" data samples. Due to the small statistics in the two data samples the plots are limited to the high mass region.

3. Efficiency and backgrounds.

Fig.7 shows the total efficiency as a function of *m*. The determination of the efficiency including all the corrections is discussed in detail in ref.[2]. Qualitatively, the efficiency is dominated by the acceptance loss for pions in the low mass region, and by the cosmic veto loss at higher masses. The

sharp drop close to the upper edge of the kinematically allowed region, is due to the drop of the photon detection efficiency.

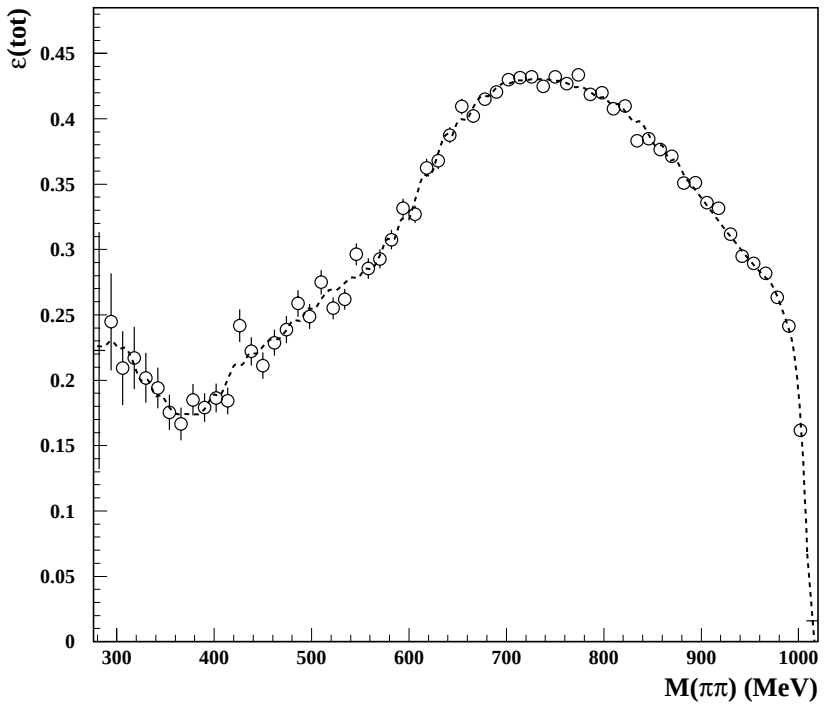

Figure 7. Total efficiency as a function of *m*.

In the higher mass region, systematic uncertainties due to the data-Montecarlo differencies in the photon measurement linearity (see [2]) are added in quadrature to the statistical uncertainties in the fit.

Among the possible backgrounds the following have been considered: (1) $\phi \rightarrow \pi^+\pi^-\pi^0$, (2) $e^+e^- \rightarrow \mu^+\mu^-\gamma$ and (3) $e^+e^- \rightarrow \pi^+\pi^-$. Fig.8 shows the estimated amount of these backgrounds at the final stage of the analysis compared to the data spectrum at the same analysis level. Backgrounds (2) and (3) are essentially negligible at the final stage of the analysis. Background (1) is still significant only in the low mass region of the spectrum.

As discussed in [2], in order to obtain an agreement between data and Montecarlo at a previous stage of the analysis, before the requirement of the photon as an energy cluster in the calorimeter, the amount of background (1) has to be multiplied by 0.47, while background (3) is correctly normalized. Moreover below 420 MeV further backgrounds not considered here appear to be significant. The fits do not include this low mass region.

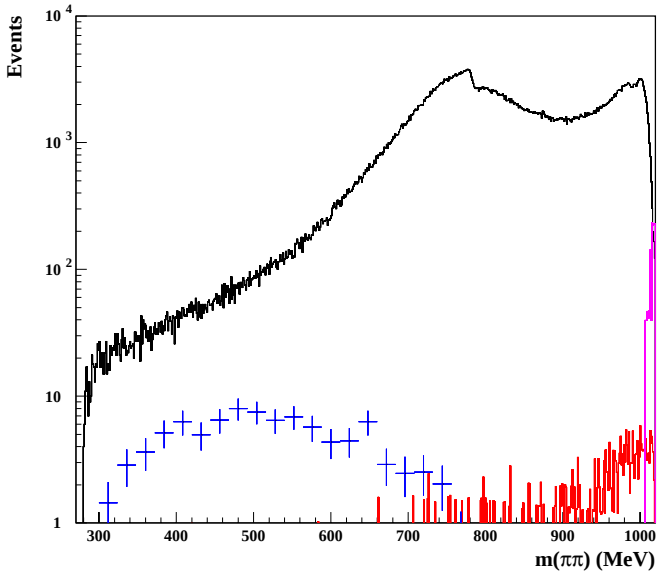

Figure 8. "On-peak" data spectrum compared in logarithmic scale to the estimated backgrounds: $\pi^+\pi^-\pi^0$ (blue), $\mu^+\mu^-\gamma$ (red) and $\pi^+\pi^-$ (purple). All the backgrounds are normalized to the total integrated luminosity.

4. Description of the scalar amplitudes used in the fit.

The description of the amplitude of the process $\phi \rightarrow S\gamma \rightarrow \pi^+\pi^-\gamma$ requires the treatment of the coupling of the ϕ to the scalar meson (the overlap of the two wave-functions).
The amplitude is:

$$A(e^+e^- \rightarrow \phi \rightarrow S\gamma \rightarrow \pi^+\pi^-\gamma) = -\frac{esm_\phi^2}{4 f_\phi D_\phi(s)}\{M\}$$

where $e=(4\pi\alpha)^{1/2}$ is the electron charge, s is the square of the center of mass energy, m_ϕ is the ϕ mass, f_ϕ is the ϕ decay constant (f_ϕ=13.1) defined by the

$$\Gamma(\phi \rightarrow ee) = \frac{4\pi\alpha^2 m_\phi}{3 f_\phi^2}$$

and $D_\phi(s)$ is the ϕ inverse propagator:

$$D_\phi(s) = m_\phi^2 - s - i\sqrt{s}\Gamma_\phi$$

with Γ_ϕ the ϕ meson width. {M} is the model dependent part of the amplitude corresponding to the red circle in fig.9. The factors before {M}, describe the coupling of the ϕ to the virtual photon originated by the e^+e^- collision, and the ϕ propagation.
The following models are considered.
(1) The Kaon-loop model (KL), mostly due to N.N.Achasov [4-5], describes the coupling of the scalar to the ϕ as a coupling of the ϕ to a kaon pair, and a subsequent coupling of the scalar to the pion pair of the final state. The $\pi\pi$ invariant mass spectrum is described introducing 3 parameters for each scalar meson: its mass and the two coupling constants to $\pi\pi$ and to KK ($g_{S\pi\pi}$ and g_{SKK} having both the dimensions of an energy).

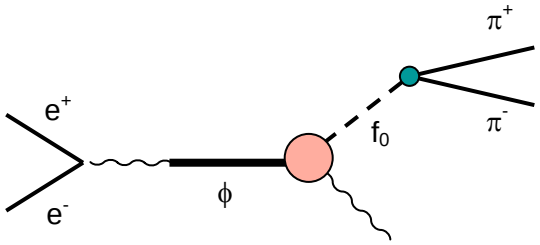

Figure 9. Diagram showing the decay $\phi \rightarrow f_0(980)\gamma \rightarrow \pi^+\pi^-\gamma$. The coupling of the ϕ to the $f_0(980)$ is contained in the red circle that is described as a kaon-loop in the KL approach and as a direct coupling in the NS approach.

(2) The No-Structure model (NS), suggested by G.Isidori and L.Maiani [6], introduces a direct coupling $g_{\phi S\gamma}$ of the ϕ to the scalar and a subsequent coupling $g_{S\pi\pi}$ of the scalar to the $\pi\pi$ pair. In this approach the scalar is described as a Breit-Wigner amplitude with a mass depending width [7]. A continuum polynomial background is added to allow the damping of the resulting curve. Parameters are: the mass of the scalar, the product $g_{\phi S\gamma} \times g_{S\pi\pi}$ the "Flatte'-like" couplings $g_{\pi\pi}$ and g_{KK} and two complex coefficients (a_0 and a_1 with the two phases b_0 and b_1) describing the background.

(3) The Scattering Amplitudes model (SA), based on the approach of M.E.Boglione and M.Pennington [8], describes the scalar amplitude as a combination of the two fundamental amplitudes $T_{11}=T(\pi\pi\rightarrow\pi\pi)$ and $T_{12}=T(KK\rightarrow\pi\pi)$ that are parametrized according to independent experimental informations. A polynomial in m^2 multiplies each fundamental amplitude. The resulting amplitude allows to extract the coupling g_ϕ with the dimensions of an energy.

The amplitude M in the frameworks defined above is given by:

$$M_{KL} = 2g(m^2)e^{i\delta(m)}\sum_{S,S'}\left(g_{SKK}G^{-1}_{SS'}g_{S'\pi+\pi-}\right)$$

$$M_{NS} = (s-m^2)\left[\frac{g_{f\pi+\pi-}g_{\phi f\gamma}}{D'_f(m^2)} + \frac{a_0}{m_\phi^2}e^{ib_0\sqrt{m^2/4-m_\pi^2}} + a_1\frac{m^2-m_f^2}{m_\phi^4}e^{ib_1\sqrt{m^2/4-m_\pi^2}}\right]$$

$$M_{SA} = (m^2-m_o^2)(1-\frac{m^2}{s})\left[(a_1+b_1m^2+c_1m^4)T_{11} + (a_2+b_2m^2+c_3m^4)T_{12}\right]e^{i\lambda}$$

I describe now the three amplitudes defining the symbols introduced.
(KL) $g(m^2)$ is the so called kaon loop function defined in ref.[9]; $\delta(m)=\theta(m^2-4m^2_\pi)^{1/2}$ is a parametrization of the final state scattering including a parameter θ that is fixed to fit the $\pi\pi$ scattering data in order to allow the amplitude to have the correct phase behaviour all over the m spectrum ($\theta = 1.47 \pm 0.14$ rad/GeV); $G_{SS'}$ is the matrix

$$G_{SS'}(m) = \begin{pmatrix} D_S(m) & -\Pi_{SS'}(m) \\ -\Pi_{S'S}(m) & D_{S'}(m) \end{pmatrix}$$

with $D_S(m^2)$ and $D_{S'}(m^2)$ the inverse propagators of the two scalars (S and S' are the two scalars) and $\Pi_{SS'}(m)$ the mixing term. The two propagators include the finite-width corrections (see [5] and [9]) taking into account the opening of the K^+K^- and K^0K^0 thresholds (that in the case of the $f_0(980)$ are very close to the resonance position). The amplitude depends on the scalar masses and couplings. A further real parameter $C_{SS'}$ is introduced in the mixing term to account for possible extra mixing schemes of the two scalar mesons.
If the second meson S' is not present, the KL M amplitude becomes:

$$M_{KL} = 2g(m^2)e^{i\delta(m)}\frac{g_{fKK}g_{f\pi+\pi-}}{D_f(m)}$$

(NS) In this case the inverse propagator is:

$D'_f(m) = m^2 - m_f^2 + im\Gamma(m)$

with the mass dependent width given by:

$$\Gamma(m) = \left[g_{\pi\pi}\sqrt{m^2/4 - m_\pi^2} + g_{KK}\left(\sqrt{m^2/4 - m_{K0}^2} + \sqrt{m^2/4 - m_{K\pm}^2}\right)\right]\frac{m_f^2}{m^2}$$

The two "Flatte'-like" parameters $g_{\pi\pi}$ and g_{KK} are adimensional and are related to the f_0 couplings through the relations:

$$g_{f\pi\pi} = \sqrt{8\pi m_f^2 g_{\pi\pi}}; g_{f\pi+\pi-} = \sqrt{2/3}\, g_{f\pi\pi}$$

$$g_{fKK} = \sqrt{8\pi m_f^2 g_{KK}}$$

The g_{KK} terms in Γ(m) become imaginary once *m* goes through the two thresholds $2m_{K0}$ and $2m_{K\pm}$. The amplitude is written in such a way to be real at the two-pion threshold $m=2m_\pi$. A further relation between the parameters is imposed, to make the slope of the phase δ^0_0 consistent with the chiral perturbation theory prediction at the two-pion threshold:

$$\frac{d\delta_0^0}{d\rho_\pi} = \frac{a_0^0}{m_\pi}$$

where $a^0_0 = 0.220$ is the pion scattering length [10] and:

$$\rho_\pi = \sqrt{\frac{m^2}{4} - m_\pi^2}$$

This condition fixes the phase b_0 to a function of the all the other parameters.

(SA) The amplitudes T_{11} and T_{12} are the results of a new still unpublished analysis [11] of ππ and πK scattering data. In these amplitudes the f_0 pole is present at $m_f = 997.21 - i\ 12.79$ MeV. The amplitude respects the gauge invariance through the $(1-m^2/s)$ term. Other than the coefficients of the polynomials (of 3rd order) two further free parameters are an overall phase λ and m_0.

5. The fits.

The "on-peak" *m* spectrum dN/d*m* with N the number of events in the bin, is fitted according to the formula:

$$\frac{dN}{dm} = \left\{\begin{array}{l}\left(\frac{d\sigma}{dm}\right)_{ISR} + \left(\frac{d\sigma}{dm}\right)_{FSR} + \left(\frac{d\sigma}{dm}\right)_{\rho\pi} \\ + \left(\frac{d\sigma}{dm}(|A|^2)\right)_{Scalar} + \left(\frac{d\sigma}{dm}(A)\right)_{\text{int.}Scalar+FSR}\end{array}\right\} \times \varepsilon(m) \times L + back(\pi^+\pi^-\pi^0 + \mu^+\mu^-\gamma)$$

here *ε(m)* and L rapresent the overall efficiency and the integrated luminosity respectively while the term *back* is the remaining contributions of the non $\pi^+\pi^-\gamma$ final states, that is held constant. For the $\pi^+\pi^-\pi^0$ contribution to *back*, the overall factor 0.47 has been applied. The other terms in the sum are the physical contributions to the $\pi^+\pi^-\gamma$ final states. By ISR and FSR I mean initial and final state radiation respectively, ρπ is the contribution of the decay chain $\phi \rightarrow \rho^+\pi^- \rightarrow \pi^+\gamma\pi^-$ plus its charge conjugated. For the first 3 terms formulas (3) to (8) of [2] are still used. 5 parameters are free: the mass and width of the ρ^0 meson; the parameters α and β describing the pion form factor according

to ref.[12]; a coefficient $a_{\rho\pi}$ that gives the size of the $\rho\pi$ contribution normalized in such a way that a value of 1 corresponds to the expected size of the contribution. Possible interference patterns of the $\rho\pi$ contribution with FSR and with the scalar part are neglected. In the following the sum of all these terms (the first line of the formula above) are called the background. It is important to stress the need to let free the background parameters. Infact the knowledge of these parameters is too poor to allow us to fix them.
The last 2 terms depend on the model for the scalars through the amplitude A defined above. For the scalar+FSR interference term, the scheme of ref.[4] is considered replacing for each fit the correct amplitude A. Radiative corrections to the scalar cross-section are applied according to ref.[4] that provides the function $H_{rad}(s)$.
No extra parameter to adjust the absolute scale is applied.
In the following I describe separately the results of the fit in the framework of the models described above. In any case the fit is done in the mass range between 420 and 1010 MeV divided in 490 bins of 1.2 MeV each. No smearing correction is applied, the mass resolution is expected to be of 1.2 – 1.4 MeV all over the mass spectrum (see [2]). On each point the uncertainty is the square root of the counting rate. On the points exceeding 1000 MeV as already said, the systematic uncertainty due to the data-MC difference in reproducing the calorimeter response is added in quadrature.

5.1 KL model without $f_0(600)$

In the KL approach, assuming that the effect of the $f_0(600)$ (if it exists) is negligible, the scalar amplitude depends only on 3 parameters related to the $f_0(980)$:

$g^2_{f0KK}/4\pi$ is the coupling of the f_0 to the kaon pair;
$R = g^2_{f0KK}/g^2_{f0\pi+\pi-}$ is the ratio of the couplings;
m_{f0} the f_0 mass.

The fit is done in the hypothesys of "destructive interference", that is the interference term is subtracted. Adding the interference term gives a very bad χ^2 probability. Moreover the parameter θ related to the final state $\pi\pi$ scattering is fixed to the value of 1.47 rad/GeV. This fit tests the hypothesis that a single scalar resonance coupled to the ϕ through a kaon loop describes the full spectrum.
Fig. 10 shows the fit results. The χ^2 probability of the fit is 4.2%. The scalar signal is given by the difference between the two curves in plots (a) or (c). Only about 25,000 events out of the 670,000 of the full spectrum, that is less than 4%, are related to the signal. In the region of the peak (between 960 and 980 MeV) the signal to background ratio reaches a maximum value of 20%. The profile of the residuals (plot (c)) has a smooth behaviour.
The results for the parameters are given in Tab.1.

Tab.1. Fit results using the KL model. The MINUIT uncertainties provided by the MINOS algorithm are reported

χ^2/ndf	538/483 (p=4.2%)		
m_{f0} (MeV)	983.0±0.6	m_ρ (MeV)	773.1±0.2
$g^2_{f0KK}/4\pi$ (GeV^2)	2.76±0.13	Γ_ρ (MeV)	144.0±0.3
R	2.66±0.10	α (x10^{-3})	1.65±0.05
		β (x10^{-3})	-123±1
		$a_{\rho\pi}$	0.0±0.6

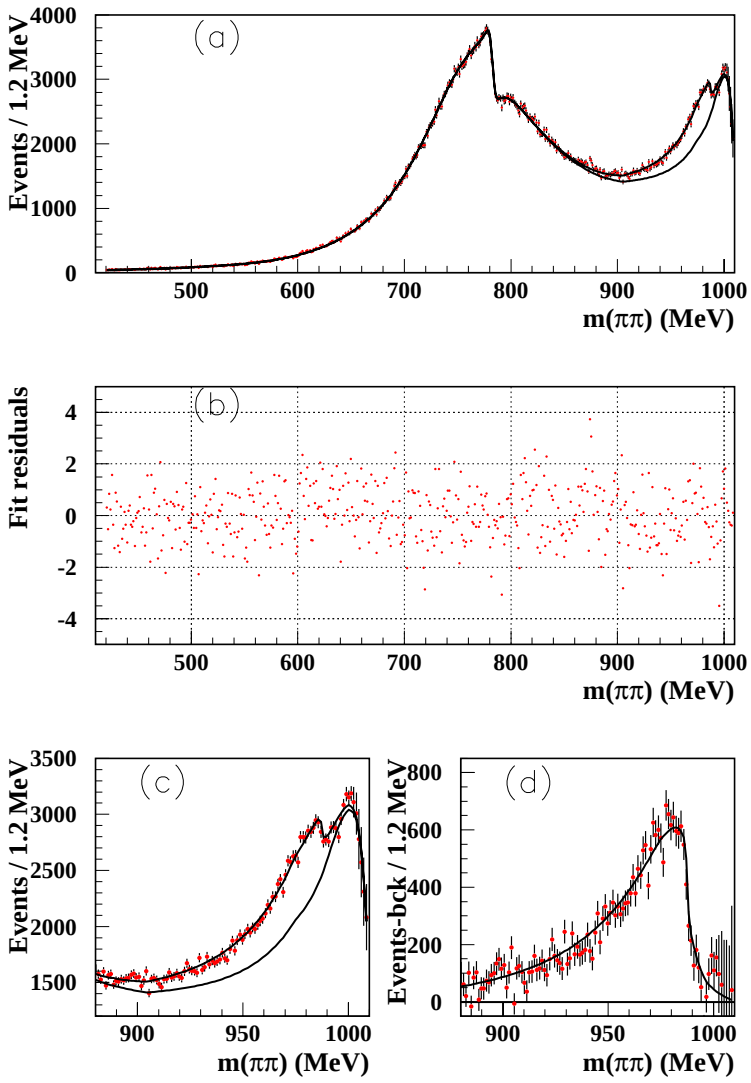

Figure 10. KL model with one single scalar fit result. (a) Data spectrum compared with the fit function and with the estimated background; (b) residuals of the fit as a function of *m*; (c) zoom on the region of the f0(980) signal; (d) data - estimated background compared to the fitting function

The scalar amplitude obtained is plotted in fig.11. Notice the phase behaviour from the two-pion threshold up to the ϕ mass.

Systematic uncertainties on the parameters are evaluated by repeating the fit in several different conditions. The results of this study is reported in Tab.2. $\sqrt{s}$ ±0.5 MeV means that I have changed the value of $\sqrt{s}$ in the fitting function; Abs.scale ± 2% means that the fitting function has been multiplied by 0.98 and 1.02 respectively. Then there are the fits done on subsamples, the one with the phase θ free (the preferred value from the fit is not compatible with 1.47, the value fixed in the baseline fit) and the fits done by using a double bin size, by changing the start and end points of the fit, by changing by a factor 2 the amount of the $\pi^+\pi^-\pi^0$ background. All the fits are done fixing the non-scalar part parameters to the baseline values. In the last row I report the result of the fit using as non-scalar part, the parameters obtained by the baseline NS fit.

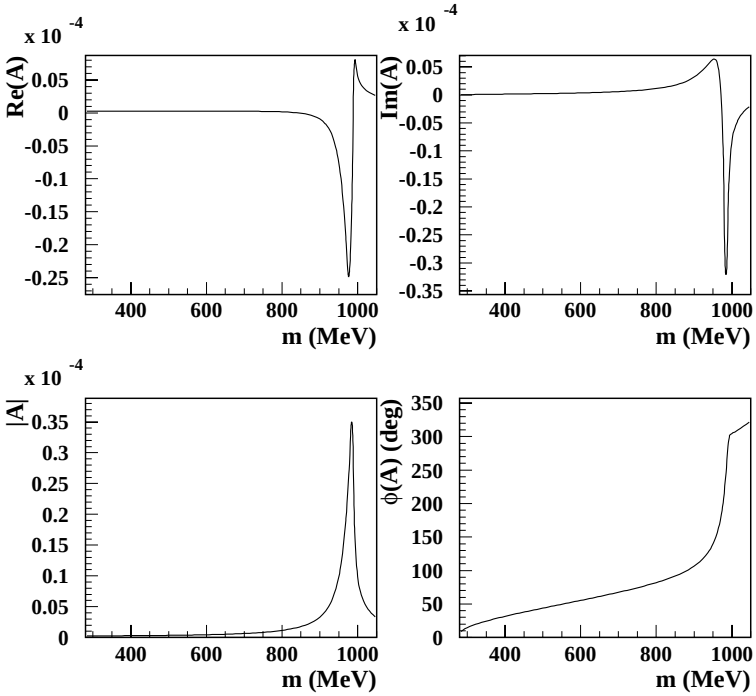

Figure 11. Behaviour of the KL amplitude resulting from the fit. Real and imaginary part are shown as a function of *m*, together with the modulus and the phase. The amplitude plotted here includes the function *g(m)* that is purely imaginary in the region of the f_0 pole.

Tab.2 Study of the systematics of the KL fit. For each fit the values of the 3 parameters are reported.

Fit	m_{f0} (MeV)	$g^2_{f0KK}/4\pi$ (GeV^2)	R
√s +0.5 MeV	982.5	2.88	2.77
√s -0.5 MeV	983.7	2.62	2.54
Abs.scale + 2%	985.2	2.52	2.64
Abs.scale - 2%	980.4	2.92	2.65
2001 data (115 pb^{-1})	979.3	1.44	2.17
2002 data (234 pb^{-1})	982.7	2.55	2.58
θ free ➔ θ = 2.3±0.2	983.0	2.76	2.66
bin = 2.4 MeV	983.5	3.12	2.76
start = 492 MeV	983.2	2.85	2.69
start = 564 MeV	983.6	3.16	2.77
end= 1002 MeV	983.0	2.75	2.66
2 × [π+π−π0 back]	981.9	2.23	2.50
0.5 × [π+π−π0 back]	983.5	3.06	2.74
NS background	987.2	2.01	2.22

These systematic studies show clearly that the signal parameters are affected by systematic uncertainties larger than the statistical uncertainties coming from the fit. This can be easily

understood given the fact that the signal to background ratio is very small for most of the *m* spectrum.
Taking the maximal variations of the parameters, we see that $g^2_{f0KK}/4\pi$ is affected by a ~ 20% systematic uncertainty while R is more stable. The larger discrepancies come from the fits done on the low statistics data samples (2001 and $\sqrt{s}$=1019.33) where larger unstabilities appear. The value of the mass is really well stable at the few MeV level. Tab.3 summarizes the results giving maximal intervals.

Tab.3 Maximal intervals of the 3 KL parameters according to the systematic studies shown in Tab.2.

m_{f0} (MeV)	980 ÷ 987
$g^2_{fKK}/4\pi$ (GeV^2)	2.0 ÷ 3.2
R= $g^2_{fKK}/g^2_{f\pi+\pi-}$	2.2 ÷ 2.8

5.2 KL model with $f_0(600)$

The insertion of a second scalar meson (that we call here the σ) in the scalar amplitude corresponds to add 4 more parameters (see above):

$g^2_{\sigma KK}/4\pi$ is the coupling of the σ to the kaon pair;
$g^2_{\sigma\pi+\pi-}/4\pi$ is the coupling of the σ to the final state pion pair ;
m_σ the σ mass;
$C_{f0\sigma}$ is a mixing parameter entering in the function $\Pi_{SS'}(m)$.

First I have tried to fit fixing m_σ to either 541 MeV or to 478 MeV, the values of the σ mass recently reported by BES [13] and E791 [14] respectively. In both cases the fit converges to values of the couplings compatible with 0, with no significant changes of the other parameters.
Letting free m_σ, the large number of free parameters makes the fit more unstable and depending on the starting points of the parameters. Several minima with similar values of the χ^2 can be obtained having completely different parameters corresponding to different interpretations. The general trend is the attempt to find a description of narrow structures as interference patterns between the $f_0(980)$ and the σ. The structures found are not statistically significant. Larger samples will help in this search.

5.3 NS model.

Other than the "background" parameters, free parameters of the fit are:

m_{f0} ,the $f_0(980)$ mass;
$g_{\phi f\gamma} \times g_{f\pi+\pi-}$,the product of the couplings;
$g_{\pi\pi}$ and g_{KK}, the "Flatte'-like" parameters;
a_0 , a_1 and b_1, the coefficients and one phase of the polynomial background: the other phase b_0 is a function of the other parameters according to [15].

A good fit is obtained with a $p(\chi^2)$ = 4.4%. Even in this case the interference term is subtracted (adding it gives a very bad χ^2 probability).
The result of the fit is shown in fig.12 and the parameters are given in Tab.4.

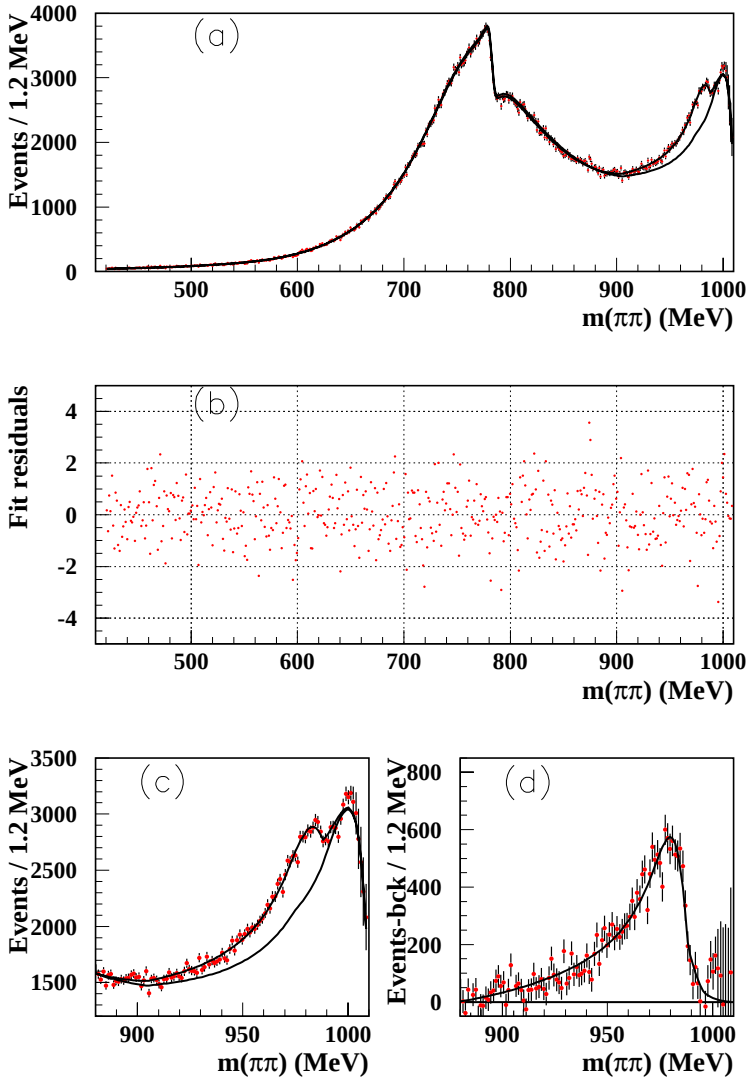

Figure 12. Same as fig. 10 for the NS fit

Tab.4. Results of the NS fit. Again the uncertainties on the parameters are given by MINOS.

χ^2/ndf	533/479 (p=4.4%)		
m_{f0} (MeV)	977.3±0.9	m_ρ (MeV)	773.0±0.1
$g_{\phi f\gamma} \times g_{f\pi+\pi-}$	1.29±0.02	Γ_ρ (MeV)	145.1±0.1
$g_{\pi\pi}$	0.057±0.002	α (x10^{-3})	1.64±0.04
g_{KK}	0.102±0.005	β (x10^{-3})	-137±1
a_0	6.00±0.02	$a_{\rho\pi}$	1.5±1.4
a_1	4.10±0.04		
b_1 (rad/GeV)	3.13±0.05		

The background parameters are comparable with those obtained with the KL fits apart from β that is appreciably larger (in absolute value) than the one obtained in the KL fit, resulting in a higher background level below the f_0 peak and consequently a lower signal size. The f_0 mass is ~ 5 MeV lower respect to the KL fit. The features of the resulting scalar amplitude are shown in fig.13.

In order to evaluate the systematic uncertainties for the f_0 parameters (mass and couplings) the fit has been repeated under several slightly different prescriptions for the polynomial background.

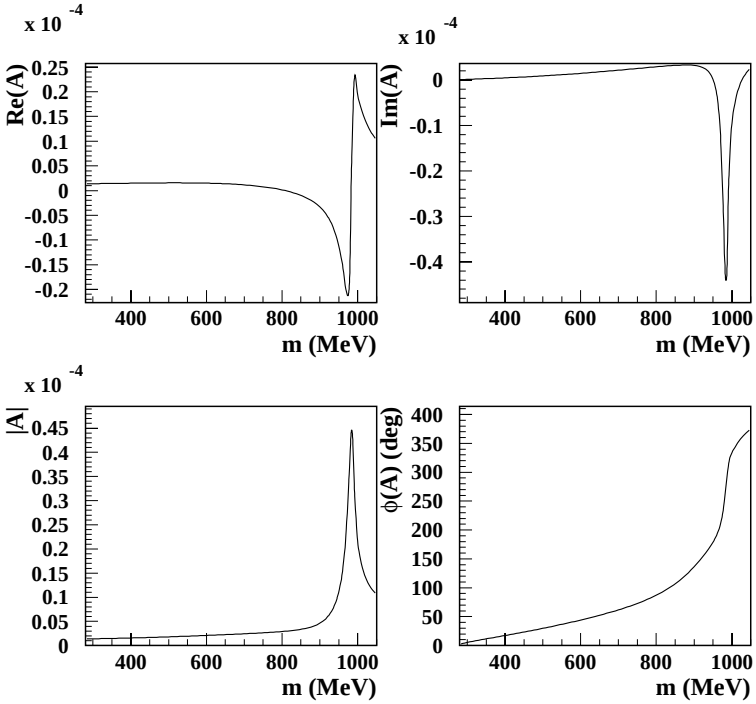

Figure 13. Behaviour of the NS amplitude resulting from the fit. Real and Imaginary part are shown as a function of *m*, together with the modulus and the phase. Compare with fig.11.

Among the prescriptions we have also tried a background where in place of the quadratic term we have added a second Breit-Wigner representing the $f_0(600)$ either with BES or E791 parameters. Again in these cases the fit becomes unacceptable and the parameters move toward a solution where $g_{KK} \sim 0$. Tab.5 shows the results of these studies.

Tab.5. Results of the study of the systematics due to the parametrisation. For each fit I report the values of the main parameters and the χ^2probability.

fit	P(χ^2)	m_{f0} (MeV)	$g_{\phi f\gamma} \times g_{f\pi+\pi-}$	$g_{\pi\pi}$	g_{KK}
no σ, b_0 constrained	4.6%	977.9	1.29	0.057	0.102
no σ, b_0 free	2.6%	978.1	1.17	0.055	0.093
no σ, $b_0 = b_1$	2.3%	978.9	1.12	0.053	0.077
no σ, $b_0 = 0$	1.2%	980.7	1.15	0.051	0.058
no σ, b_0 free $b_1 = 0$	2.3%	978.7	1.13	0.053	0.081
σ BES b_0 constrained	$\sim 10^{-7}$	983.2	0.76	0.034	<0.01
σ E791 b_0 constrained	$\sim 10^{-6}$	983.4	0.80	0.034	<0.01
σ BES b_0 free	0.1%	983.6	0.88	0.040	<0.02

σ E791 b_0 free	$\sim 10^{-5}$	983.4	0.81	0.035	<0.01

The fits 6-9 are not acceptable and are not used in the determination of the systematics.
The fits 1-5 are all equally acceptable and give comparable results for the relevant f_0 parameters. The phase of each solution has a substancially different behaviour in the intermediate *m* region, say between 500 and 900 MeV. This means that the f_0 parameters are quite independent from the details of the amplitude in the intermediate region where the background dominates.
Further systematic checks (the same done for the KL fit) are given in Tab.6.

Tab.6. Results of the systematics studies for the NS fit. For each fit the values of the physical couplings are given directly.

fit	m_{f0} (MeV)	$g_{\phi S\gamma}$	$g_{S\pi+\pi-}$	g_{SKK}
√s +0.5 MeV	979.0	1.56	1.00	1.67
√s -0.5 MeV	976.2	1.39	0.98	1.73
Abs.scale + 2%	981.4	1.23	0.89	1.97
Abs.scale - 2%	973.0	1.74	1.09	2.29
2001 data (115 pb-1)	982.8	1.27	0.91	0.83
2002 data (234 pb^{-1})	974.7	1.56	1.03	2.01
bin = 2.4 MeV	976.5	1.50	1.00	1.82
start = 492 MeV	978.4	1.46	0.98	1.60
start = 564 MeV	978.5	1.45	0.98	1.58
end= 1002 MeV	977.2	1.48	1.00	1.74
2 × [π+π−π0 back]	977.7	1.47	0.99	1.68
0.5 × [π+π−π0 back]	976.9	1.49	1.00	1.78
KL background	977.4	2.05	1.10	2.14

As can be seen in Tab.6, the larger source of systematic uncertainty on the f0 parameters is related to the fit conditions. However, notice that due to the correlations, this uncertainty partly cancels out in the determination of $R = g^2_{SKK} / g^2_{S\pi\pi}$ and $g_{\phi S\gamma}$.
Summarizing the results of the NS fits we give the maximal intervals for the f_0 parameters accessible to this analysis in Tab.7.

Tab.7. Maximal intervals for the f0 parameters extracted with the NS fit.

m_{f0} (MeV)	973 ÷ 981
$g_{\phi S\gamma}$ (GeV^{-1})	1.2 ÷ 2.0
$g_{f\pi+\pi-}$ (GeV)	0.9 ÷ 1.1
g_{fKK} (GeV)	1.6 ÷ 2.3
$R = g_{KK} / g_{\pi\pi}$	2.6 ÷ 4.4

5.4 SA model.

Other than the usual "background" parameters the fit has 8 free parameters: the 6 coefficients of the two 3rd order polynomials, the parameter m_0 and the overall phase λ. The fit converges with a χ^2 of 577 /477 with a probability of $p(\chi^2)=1.1\ 10^{-3}$. The parameters found are listed in the Tab.8, the fit is shown in fig.14.

Tab.8 Results of the SA fit.

χ^2/ndf	577/477 (p=0.1%)		
a_1	11.9	m_ρ (MeV)	774.4±0.2
b_1	3.3	Γ_ρ (MeV)	142.8±0.3
c_1	-15.1	α (x10^{-3})	1.74±0.05
a_2	-14.7	β (x10^{-3})	-100±18
b_2	-15.3	$a_{\rho\pi}$	0±2
c_2	35.8		
m_0	0.		
λ (rad)	-1.63		

The fit is clearly worse than in the other two cases. Here the fit lowers the background in the f_0 region (compare the value of β with the one obtained in the other fits), enhancing the signal.
Using the amplitude resulting from these parameters, we found the coupling g_ϕ (see definition in [8]) to be: $6.6\ 10^{-4}$ GeV. This result is in full agreement with the value found in [8] applying the so-called re-VAMP parametrisation on $\pi^0\pi^0\gamma$ data from KLOE and SND and corresponds to a branching ratio of $\sim 3 \times 10^{-5}$.

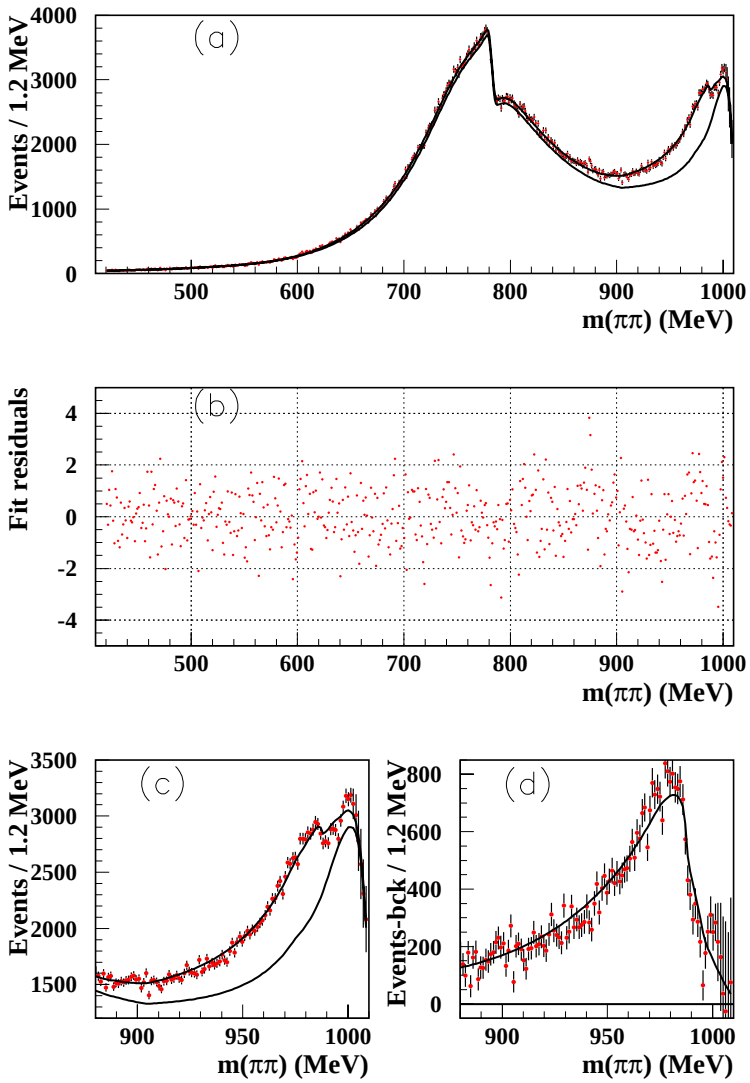

Figure 14. Same as fig.10 for the SA fit.

5.5 Comment on the background.

The sharp structure of the ρ – ω interference pattern (a ~35% drop in ~ 7 MeV) allows to test our absolute mass scale and resolution. By letting free the ω mass and width in the fit and without any correction for the smearing, we obtain the following values:

m_ω = 782.18 ± 0.58 MeV PDG value = 782.59 ± 0.11 MeV

Γ_ω = 8.87 ± 0.84 MeV PDG value = 8.49 ± 0.08 MeV

in good agreement with PDG values at the hundreds-keV level with no appreciable variations of the other fit parameters. Fig.15 shows the detail of the fit in the ρ – ω interference region.

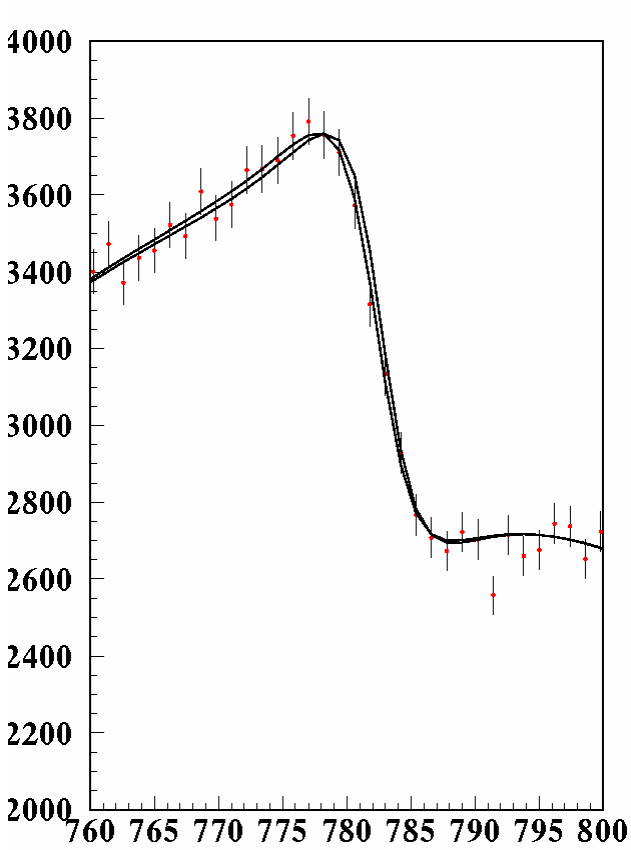

Figure 15. Detail of the KL fit in the ρ – ω interference region. The red points are the data, the two curves are the two fits with ω parameters free and fixed.

The values of the parameters of the pion form factor in the Kuhn-Santamaria parametrization are summarized in Tab.9.

Tab.9 Comparison between the Kuhn-Santamaria parameters obtained in the three fits discussed above.

	Fit KL	Fit NS	Fit SA
m_ρ (MeV)	773.1	773.0	774.4
Γ_ρ (MeV)	144.0	145.1	142.8
α ($x10^{-3}$)	1.65	1.64	1.74
β ($x10^{-3}$)	-123	-137	-100

These values can be hardly compared with other experiments or analyses because tipically are obtained with slightly different parametrizations. For instance the value of β depends on the mass and the width chosen for ρ' (I have used the PDG values m=1465 MeV, Γ=310 MeV, but other experiments use significantly different values).

6. Discussion of the results.

6.1 Line-shapes.

All the fits give similar "background" parameters, compatible with the expected values. The value of β that is the less well known, determines the size of the f_0 signal over the background. In any case the f_0 signal appears as a narrow asymmetric peak (FWHM ~ 30 MeV) with a size between 20 and 25 % of the background. Fig.16 shows the subtracted f_0 peak according to the 3 fits. The KL and NS fits interpret the observed narrow peak as due to a broad scalar shape (the term $(d\sigma/dm)_{scalar}$ that has a different shape in the two cases) strongly cancelled by the destructive interference pattern

with FSR (the term and $(d\sigma/dm)_{int.scalar+FSR}$). The SA fit prefers a much narrower shape. Fig.17 shows the line-shapes resulting from the 3 fits.

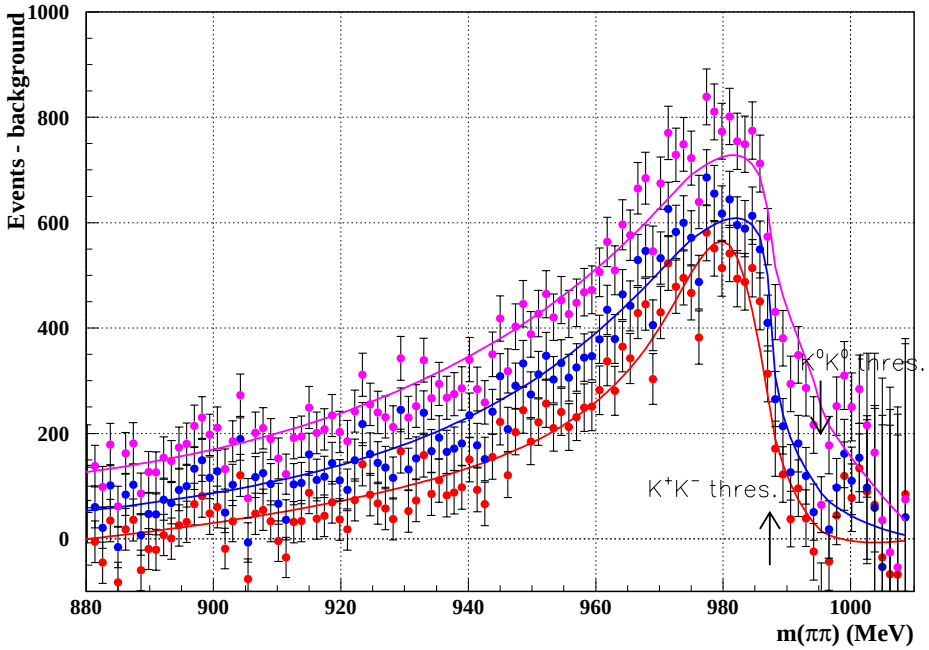

Figure 16. Subtracted f_0 spectrum according to the KL fit (blue points and curve), NS fit (red points and curve) and finally SA fit (magenta). The K^0K^0 and K^+K^- threshold positions are indicated.

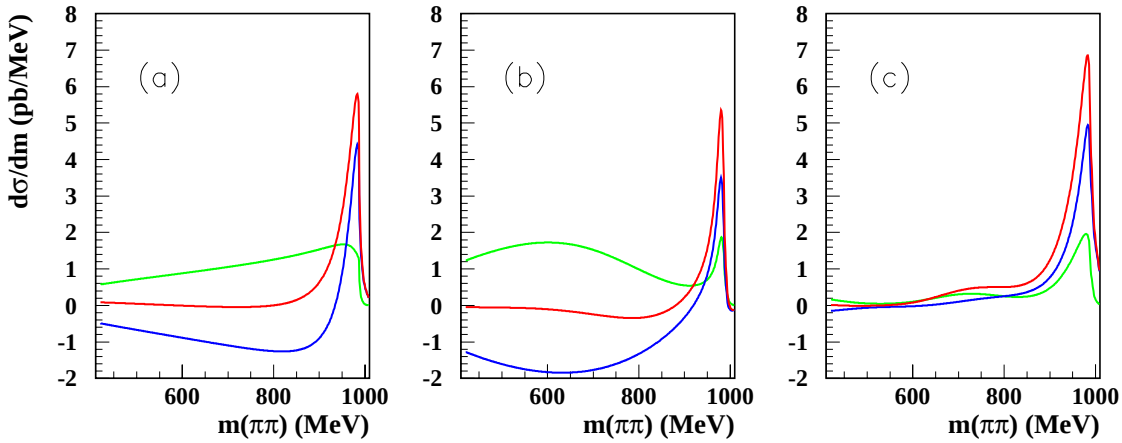

Figure 17. Terms $(d\sigma/dm)_{scalar}$ (green), $(d\sigma/dm)_{int.scalar+FSR}$ (blue) and their sum (red) resulting from fit KL (a), NS (b) and SA (c).

The low mass region is intrinsically badly defined, due to the large unavoidable background. The $\pi^+\pi^-\gamma$ final state allows to see the f_0 peak and to study its parameters, but is not the best place to study the low mass behaviour of the scalar amplitude.

Finally few remarks concerning the phase behaviour of the resulting amplitude. By comparing the behaviours of $\phi(A)$ in figs.11 and 13 we see that in both cases the phase is 0 at the $\pi\pi$ threshold, then it rises almost linearly, and finally at the f_0 peak passes through ~3/2 π. In the KL model this can be easily understood. Infact at the f_0 pole $\phi(1/D_f(m_f)) \sim \pi/2$, $\delta(m_f) \sim \pi/2$ and finally $\phi(g(m_f))$ is also $\sim \pi/2$. By removing the kaon-loop function g(m) we recover the familiar $\pi\pi$ scattering phase behaviour that reaches $\sim \pi$ at the f_0 pole. In the NS model again $\phi(1/D'_f(m_f)) \sim \pi/2$ and the extra π is provided by the background (you can see that b_1 tipically is close to π rad/GeV).

6.2 f_0 couplings.

We get 3 couplings: $g_{\phi f0\gamma}$, $g_{f0\pi+\pi-}$ and g_{f0KK}. Here I summarize all the fit campaign allows us to say about the couplings.

In several papers (for instance ref.[9]) it was pointed out that the relevant information to give is the branching fraction of $\phi \rightarrow f_0\gamma \rightarrow \pi^+\pi^-\gamma$. In the context of this analysis the definition of this branching ratio is not straightforward. Infact we have amplitudes of processes that give rise to the same final states. No branching fraction defined as the ratio between two counting rates can be defined. Better is to directly give the coupling $g_{\phi f0\gamma}$. For the NS fit, $g_{\phi f0\gamma}$ multiplied by $g_{f0\pi+\pi-}$ is a parameter of the fit and the disentangling between the 2 couplings can be done extracting $g_{f0\pi+\pi-}$ by the value of $g_{\pi\pi}$ as we have already done in sect.5.3. For the KL fits the coupling $g_{\phi f0\gamma}$ can be obtained using the definition of the coupling in terms of the partial width that gives:

$$g_{\phi f0\gamma} = \left[\frac{3}{\alpha} \left(\frac{2m_\phi}{m_\phi^2 - m_{f0}^2} \right)^3 \Gamma_\phi \text{"}BR\text{"} \frac{1}{F} \right]^{1/2}$$

where all the symbols are defined apart from F that is the fraction of f_0 decaying to $\pi^+\pi^-$ respect to the total width (=2/3 for $\pi^+\pi^-$ and =1/3 for $\pi^0\pi^0$) and "BR" that is the equivalent branching ratio, defined as the integral of the scalar term on the full *m* spectrum normalized to the total ϕ production cross-section:

$$\text{"BR"} = \frac{1}{\sigma(\phi)} \int \left(\frac{d\sigma}{dm} (|A|^2) \right)_{scalar} dm .$$

By integrating the function resulting from the KL fit we get BR=2.1×10^{-4}.

The value of $g_{\phi f0\gamma}$ is particularly interesting becuase it can be directly compared to the same coupling of the ϕ to the pseudoscalar mesons π^0, η and η' that have a quite well defined quark composition.

All the relevant couplings extracted from this analysis are summarized in Tab.10 where the values obtained in the baseline fits are reported together with the maximal ranges according to the discussion of the systematic uncertainties given in sect.5.

Tab.10. Summary of the couplings obtained in the fits discussed above.

	KL without $f_0(600)$	NS
g_{f0KK} (GeV)	5.0 ÷ 6.2	1.6 ÷ 2.3
$g_{f0\pi+\pi-}$ (GeV)	3.0 ÷ 4.2	0.9 ÷ 1.1
$R=(g_{f0KK} / g_{f0\pi+\pi-})^2$	2.2 ÷ 2.8	2.6 ÷ 4.4
$g_{\phi f0\gamma}$ (GeV^{-1})	3.5	1.2 ÷ 2.0

First we look at the couplings of the f_0 to kaons and pions. Both fits support a larger coupling of the f_0 to the kaons than to the pions. On the other hand the KL fit gives couplings that are a factor ~4 larger than those of the NS fit. This large difference can be explained as follows: according to the KL model the scalar amplitude is entirely due to the f_0 couplings, while in the NS approach the f_0 accounts only for a part of it, the large tail being due to the polynomial background.

For what concern $g_{\phi f0\gamma}$ we found again a large discrepancy between the 2 fits. It is anyhow interesting to compare the values found with the same couplings to the ϕ of the pseudoscalar mesons reported in the Tab.11. Whatever is the approach used in the fit, the f_0 coupling is larger than any of the pseudoscalar couplings.

Tab.11. Coupling of the f to the accessible pseudoscalar mesons. Compare with the last line of Tab.10.

Meson	$g_{\phi M\gamma}$ (GeV^{-1})
π^0	0.12
η	0.66
η'	0.70

In conclusion, both fits indicate clearly a strong coupling of the f_0 to the strange quarks.

6.3 Is there any σ?

In the KL framework, a reasonable fit is obtained with $f_0(980)$ only (see sect.5.1) with a χ^2 probability of 3.7%. There is no space for an inclusion of an $f_0(600)$ meson with BES or E791 parameters.
In the NS approach the background in the scalar amplitude is well described by a second order polynomial. Trying to force it to a Breit-Wigner like shape we get a worse fit.
The conclusion is that we are able to describe the spectrum in a satisfactory way, without introducing any further meson respect to the $f_0(980)$.
As a general remark, we observe that in this particular final state, given the large unreduceble signal, the search for a tiny effect due to the σ meson is not straightforward.

6.4 Extrapolation to "off-peak" data.

A further important test of the underlying theory is provided by the analysis of the "off-peak" data. The *m* spectra of the 2 data samples at $\sqrt{s}$ = 1017 and 1022 MeV are compared to the expected ones obtained using the parameters found in the "on-peak" KL fit and applying the same efficiency profile. The absolute comparisons are shown in fig.18. Due to the low statistics of the 2 samples, the f_0 signal is not as evident as in the on-peak data. However an acceptable agreement is found, and in the 1022 MeV data, the effect of the signal is necessary to describe the spectrum. Finally fig.19 gives the comparison of the W=$\sqrt{s}$ dependence of the 900-1000 MeV interval cross-section with absolute predictions based on the "on-peak" results for the KL fit. The data are at least qualitatively in agreement with the prediction based on the extrapolation from the "on-peak" results.

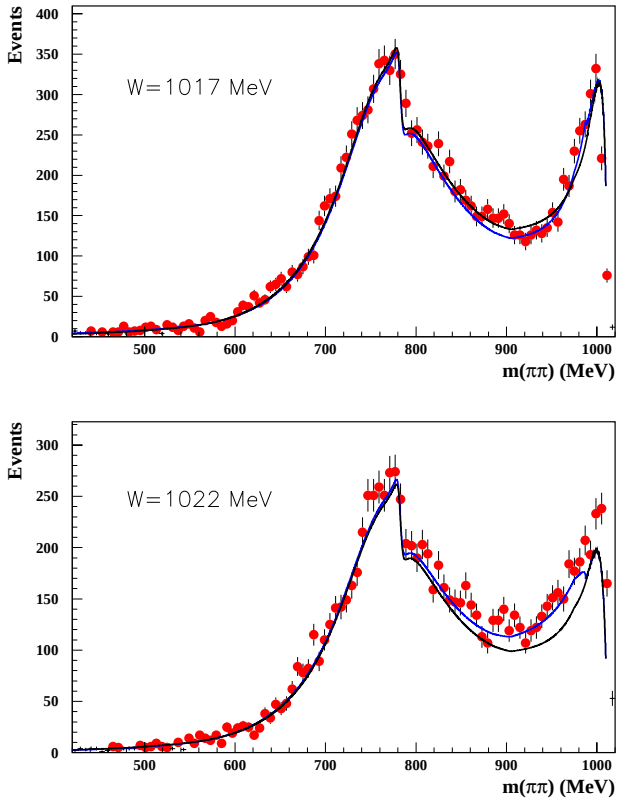

Figure 18. Mass spectrum for the two "off-peak" data samples. Red are data, blue is the expected shape of the spectrum obtained extrapolating the results obtained with KL fit on the "on-peak" spectrum. In black is the extrapolated background.

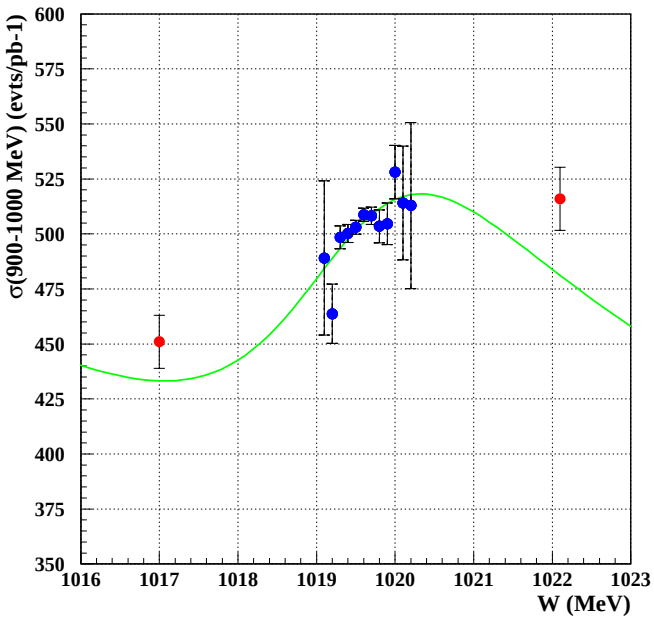

Figure 19. Same data shown in fig.4 compared with the expected center of mass dependence obtained extrapolating the results of the KL fit (green curve).

6.5 The charge asymmetry.

The behaviour of the charge asymmetry as a function of *m* (see fig.5), is compared with a simulation of $\pi^+\pi^-\gamma$ events with the same kinematical cuts based on EVA. The result of the comparison is shown in fig.20. A clear discrepancy is observed between the data and the expectations based on the interference between the ISR and FSR amplitudes only. Other than a clear discrepancy in the region of the $f_0(980)$, a very significant discrepancy in the region below 700 MeV is observed. Following the analysis of ref.[16] we have included in the EVA generator a scalar amplitude according to the results of the KL fit. As can be seen in fig.20, the new simulation is able to describe qualitatively well both the effect in the f_0 region and also the sizeable effect at low masses. Notice that the comparison between data and simulation is absolute, no parameter is adjusted based on the asymmetry plot.

The off-peak data (see fig.6) are not accurate enough to allow a comparison. In any case even with this low statistics a signal around 980 MeV can be observed in the W=1022 MeV run.

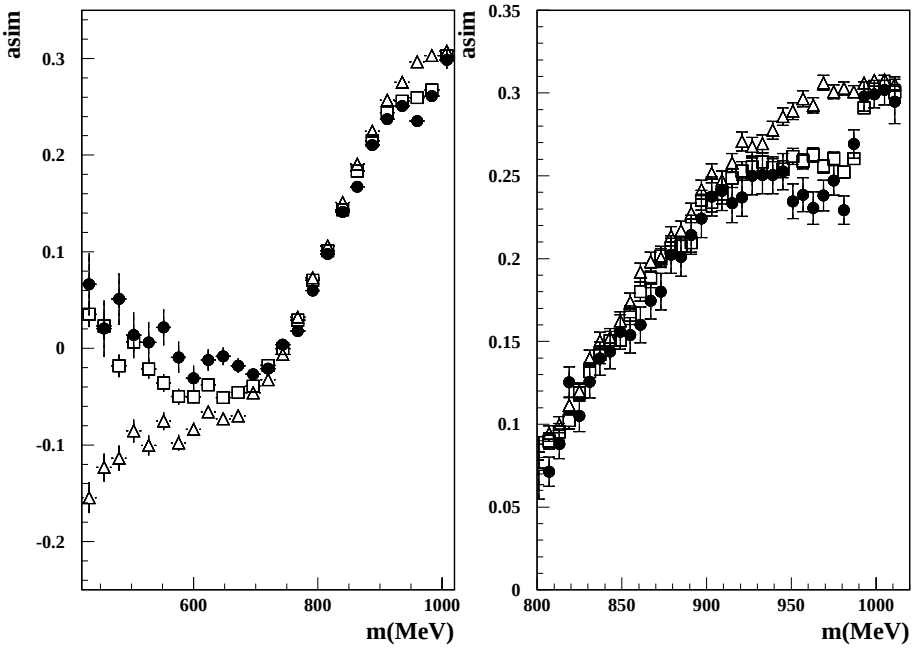

Figure 20. Same data of fig.5 (full circles) compared to the Montecarlo expectations based on ISR and FSR only (open triangles) and on ISR, FSR and KL scalar amplitude (open squares). Left plot is on the full spectrum, right plot is a zoom in the f_0 region only.

7.Conclusions.

We have found a clear evidence of the $f_0(980)$ decaying in $\pi^+\pi^-$. The signal appears as a narrow peak (FWHM of $30 \div 40$ MeV) in the dN/d*m* spectrum and in the charge asymmetry profile.

Acceptable χ^2 probabilities are obtained by fitting the dN/d*m* spectrum including a scalar amplitude where the $f_0(980)$ is described according either to the KL or the NS model. A marginally acceptable χ^2 probability is obtained using the SA model.

The $f_0(980)$ is strongly coupled to the ϕ and the coupling to kaons is larger than the coupling to pions. This is a common feature of both the KL and NS fit results.

Any attempt to include a second scalar meson with parameters fixed to the recently reported values by the E791 and BES collaborations, doesn't improve the fit.
The kaon-loop amplitude found in the fit of the spectrum describes qualitatively well the profile of the charge asymmetry.
One remark concerns the kaon-loop model. With only 3 parameters adjusted to the data, the KL amplitude is able to describe in a reasonable way the *m* spectrum, the cross-section dependence on √s and the charge asymmetry. Fig.21 shows the agreement found for the KL fit in all the variables.

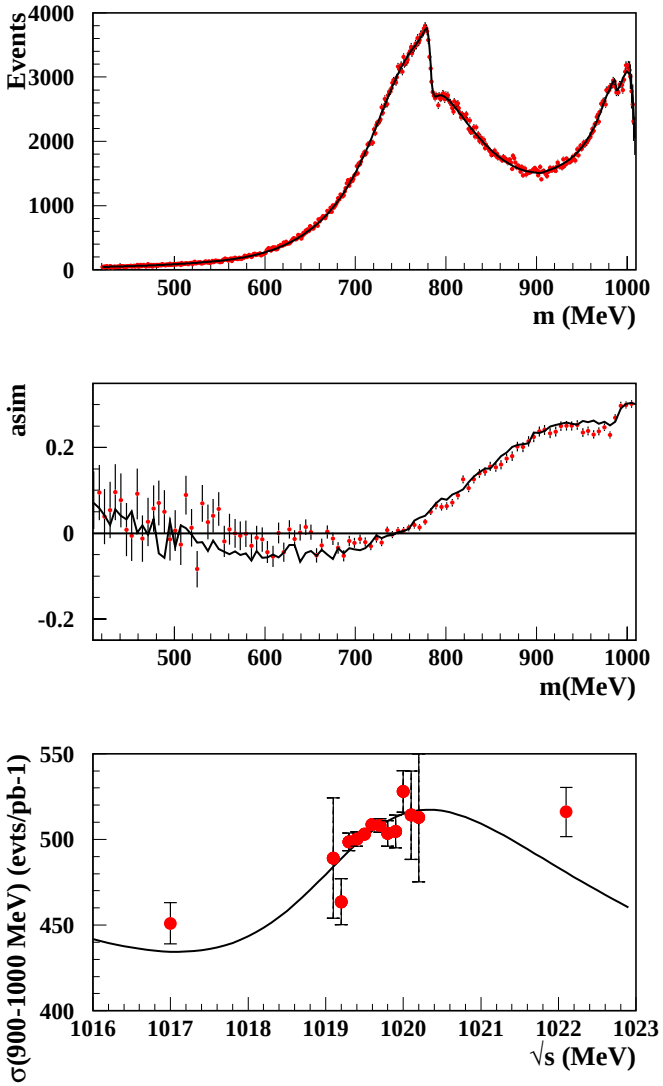

Figure 21. Summary of the comparison between data (red) and KL expectations (black). The KL model requires 3 parameters only to describe event spectrum (first plot), charge asymmetry (second plot) and √s dependence of the cross-section (third plot).

Acknowledgments

Many theoreticians and phenomenologists have contributed to all this study. In alphabetic order: N. N. Achasov, M. E. Boglione, H. Czyz, R. Escribano, G. Isidori, L. Maiani, S. Pacetti and M. R. Pennington.

References

[1] CMD-2 Collaboration, Phys.Lett.B462 (1999) 371;
[2] C.Bini, S.Ventura, KLOE Note 206 10-2005;
[3] KLOE Collaboration, Phys.Lett.B606 (2005) 12;
[4] N.N.Achasov, V.V.Gubin, Phys.Rev.D57 (1998) 1987;
[5] N.N.Achasov, V.V.Gubin, Phys.Rev.D56 (1997) 4084;
[6] G.Isidori, L.Maiani, S.Pacetti, private communication ;
[7] S.M.Flatte', Phys.Lett.B63 (1976) 224;
[8] M.Boglione, M.R.Pennington Eur. Phys. J. C30 (2003) 503;
[9] N.N.Achasov, V.N.Ivanchenko, Nucl.Phys. B315 (1989) 465;
[10] G.Colangelo, AIP Conf. Proc 756:60-69, hep-ph/0501107;
[11] M.Boglione, M.R.Pennington, in preparation;
[12] J.H.Kuhn, A.Santamaria, Z.Phys.C48 (1990) 445;
[13] BES; M.Ablikim et al., Phys.Lett.B598 (2004) 149;
[14] E791; E.M.Aitala et al., Phys.Rev.Lett. 86 (2001) 770;
[15] S.Pacetti, in preparation;
[16] H.Czyz, A.Grzelinska, J.H.Kuhn, hep-ph/0412239.